

Modular Focusing Ring Imaging Cherenkov Detector for Electron-Ion Collider Experiments[☆]

C.P. Wong^{g,*}, M. Alfredⁱ, L. Allison¹, M. Awadiⁱ, B. Azmoun^c, F. Barbosa^m, J. Bennett^g, W. Brooks^q, T. Cao^h, M. Chiu^c, E. Cisbani^{k,l}, M. Contalbrigo^j, A. Datta^s, A. Del Dotto^{k,t}, M. Demarteau^b, J.M. Durhamⁿ, R. Dzhigadlo^h, T. Elder^g, D. Fields^s, Y. Furletova^m, C. Gleason^t, M. Grosse-Perdekamp^r, J. Harris^f, T. Hasler^g, X. He^g, H. van Heckeⁿ, T. Horn^d, A. Hruschka^g, J. Huang^c, C. Hyde^f, Y. Ilieva^t, G. Kalicy^d, M. Kimball^a, E. Kistenev^c, Y. Kulinich^r, M. Liuⁿ, R. Majka^f, J. McKisson^m, R. Mendezⁿ, P. Nadel-Turonski^p, K. Park^m, K. Peters^h, T. Rao^c, R. Pisani^c, Yi Qiang^m, S. Rescia^c, P. Rossi^m, O. Sarajlic^g, M. Sarsour^g, C. Schwarz^h, J. Schwiening^h, C.L. da Silvaⁿ, N. Smirnov^u, H. Stien^a, J. Stevens^e, A. Sukhanov^c, S. Syed^g, A. Tate^a, J. Toh^r, C. Towell^a, R. Towell^a, T. Tsang^c, R. Wagner^b, J. Wang^b, C. Woody^c, W. Xi^m, J. Xie^b, Z.W. Zhao^f, B. Zihlmann^m, C. Zorn^m

^aAbilene Christian University, Abilene, TX 79601

^bArgonne National Lab, Argonne, IL 60439

^cBrookhaven National Lab, Upton, NY 11973

^dCatholic University of America, Washington, DC 20064

^eCollege of William & Mary, Williamsburg, VA 23185

^fDuke University, Durham, NC 27708

^gGeorgia State University, Atlanta, GA 30303

^hGSI Helmholtzzentrum für Schwerionenforschung GmbH, 64291 Darmstadt, Germany

ⁱHoward University, Washington, DC 20059

^jINFN, Sezione di Ferrara, 44100 Ferrara, Italy

^kINFN, Sezione di Roma, 00185 Rome, Italy

^lIstituto Superiore di Sanità, 00161 Rome, Italy

^mJefferson Lab, Newport News, VA 23606

ⁿLos Alamos National Lab, Los Alamos, NM 87545

^oOld Dominion University, Norfolk, VA 23529

^pStony Brook University, Stony Brook, NY 11794

^qUniversidad Técnica Federico Santa María, Valparaíso, Chile

^rUniversity of Illinois, Urbana-Champaign, IL 61801

^sUniversity of New Mexico, Albuquerque, NM 87131

^tUniversity of South Carolina, Columbia, SC 29208

^uYale University, New Haven, CT 06520

Abstract

A powerful new electron ion collider (EIC) has been recommended in the 2015

[☆]EIC Detector R&D Consortium

*Corresponding author

Email address: cwong14@student.gsu.edu (C.P. Wong)

Long Range Plan for Nuclear Science for probing the partonic structure inside nucleons and nuclei with unprecedented precision and versatility [1]. EIC detectors are currently under development [2], all of which require hadron identification over a broad rapidity coverage. A prototype ring imaging Cherenkov detector has been developed for hadron identification in momentum range from 3 GeV/c to 10 GeV/c. The key features of this new detector are compact and modular design, using aerogel and a fresnel lens for ring imaging. In this paper, the results from a beam test of a prototype device at Fermilab are reported.

Keywords: Cherenkov radiation, Fresnel lens, Aerogel, EIC

1. Introduction

The ability to identify hadrons is a key requirement for the physics program of the EIC experiments. By tagging the flavor of the struck quark in semi-inclusive deep inelastic scattering (SIDIS), one can obtain the transverse momentum distributions of the strange sea quark, while kaons which subsequently decay from open charm are important for probing the distribution of gluons in protons and nuclei.
5

Mesons in the electron beam direction and proton beam direction will carry momenta up to 10 GeV/c and 100 GeV/c, respectively, while the meson momenta in central region are typically less than 10 GeV/c.
10

To fulfill different particle identification (PID) requirements associated with the three different kinematic regions of the EIC detectors, an R&D consortium (eRD14) has been formed to study the technology choices of ring imaging Cherenkov (RICH) detectors. A modular aerogel RICH (mRICH) detector is
15 proposed to provide PID in the momentum range from 3 GeV/c to 10 GeV/c in the electron beam direction.

2. Detector Design

The current state-of-the-art designs of imaging Cherenkov detectors, such as proximity focusing detectors [3, 4], or mirror-based imaging detectors [5–

10] occupy substantial volumes, due to requirements imposed by the optical
20 elements in the case of mirror-based detectors, or the desired ring separation in
the case of proximity focusing devices. In the endcap region of the proposed EIC
detector, such space is not available. A set of compact and modular detectors
would fit into the available space and still provide hadron PID capability with
25 momentum coverage from 3 GeV/c to 10 GeV/c.

The mRICH consists of four components. A block of aerogel serves as the
Cherenkov radiator. Immediately following is an acrylic Fresnel lens which
serves to produce a focused ring image and acts as a UV filter [11]. In the image
30 plane is a pixelated optical sensor, and the walls of the unit between the lens
and image plane are formed by four flat mirrors. The device is shown in Fig. 1.
Also shown in Fig. 1 is an event display of a 9 GeV/c pion launched toward the
center of the mRICH detector using the GEMC simulation framework that is
based on Geant4 [12].

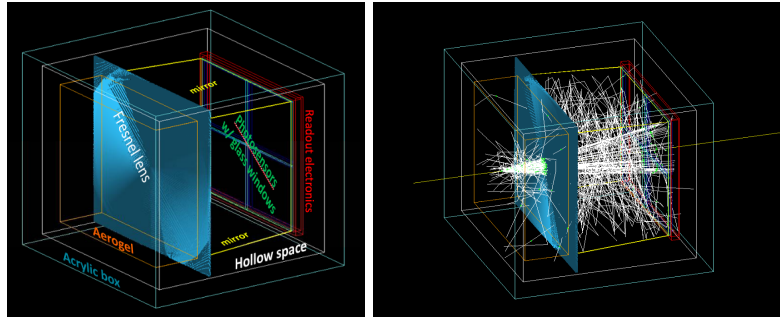


Figure 1: (left) mRICH detector and its components; (right) an event display of single 9 GeV/c pion launched toward to the center of the mRICH detector.

Figure 2 shows the focusing feature of the mRICH detector performance
35 over a proximity-focusing Cherenkov detector design. Figure 3 demonstrates
the capability of the mRICH for shifting the ring image to the central region of
the photosensor plane for non-normal incident particles. It is clear that a much
less active photosensor coverage is needed for the mRICH design in comparison
with other RICH detector designs.

The PID performance of a ring image Cherenkov detector can be characterized by separation power (or number of sigma)

$$N_\sigma = \frac{\Delta\theta\sqrt{N_{photon}}}{\sigma_\theta}, \quad (1)$$

where $\Delta\theta$ is the difference the Cherenkov angles from two different species of particles, N_{photon} is the number of photon detected, and σ_θ is the uncertainty of a single photon measurement. Sources of uncertainty of a single photon measurement are the emission point σ_{EP} , chromatic dispersion σ_{Chro} , and pixel size σ_{Det} [13]. The resulting uncertainty σ_θ for a single photon measurement is a quadrature sum,

$$\sigma_\theta = \sqrt{\sigma_{EP}^2 + \sigma_{Chro}^2 + \sigma_{Det}^2}. \quad (2)$$

⁴⁰ σ_{EP} is minimized in lens based design as a result of lens focusing property.

The first prototype of this device consists of a 3.3 cm thick aerogel block with index of refraction $n = 1.03$, a Fresnel lens with 76.2 mm (3'') focal length (from Edmund Optics, part number 32-593)[14], a mirror set mounted on top, bottom, left and right of the detector interior, and a sensor plane composed ⁴⁵ of four Hamamatsu 12700 multianode PMT arrays. The assembled mRICH prototype is shown in Fig. 4 (left). The expanded 3D rendering of the detector components are also shown on the right in Fig. 4.

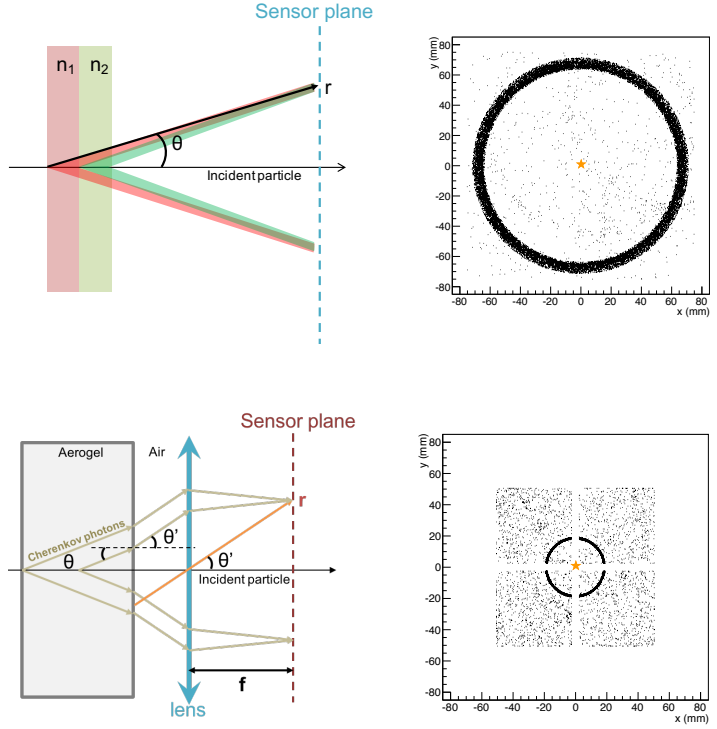


Figure 2: Comparison of the ring image characteristics between a proximity-focusing RICH (top, based the BELLE-2 ARICH detector design) and the mRICH (bottom). The ray diagrams on the left (not to scale, for illustration purposes only) show the optical properties without (top) and with focusing lens (bottom). The ring images are generated with Geant4 simulation from 100 9 GeV/c pions in both cases. The distance from the sensor plane of the proximity RICH to the mid-point of n_1 and n_2 is 20 cm. The total thickness of n_1 and n_2 is 4 cm. The focal length of the mRICH Fresnel lens is 7.6 cm and the mRICH aerogel block thickness is 3.3 cm. The blank regions in the lower left X-Y hits scatter plot are the physical separations between the photosensor modules that is only relevant to the mRICH.



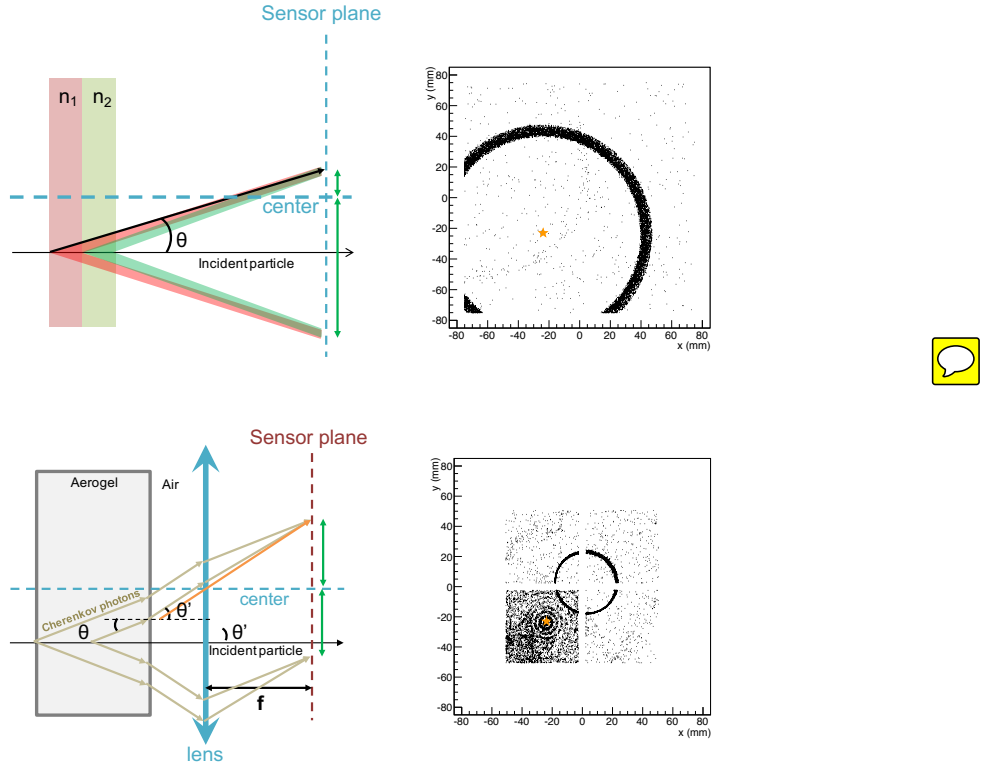


Figure 3: Comparison of the ring image location on the sensor plane between a proximity-focusing RICH (top, based the BELLE-2 ARICH detector design) and the mRICH (bottom). The ray diagrams on the left (not to scale, for illustration purposes only) show the optical properties without (top) and with focusing lens (bottom). The ring images are generated with Geant4 simulation from 100 9 GeV/c pions in both cases. The distance from the sensor plane of the proximity RICH to the mid-point of n_1 and n_2 is 20 cm. The total thickness of n_1 and n_2 is 4 cm. The focal length of the mRICH Fresnel lens is 7.6 cm and the mRICH aerogel block thickness is 3.3 cm. The blank regions in the lower left X-Y hits scatter plot are the physical separations between the photosensor modules that is only relevant to the mRICH.

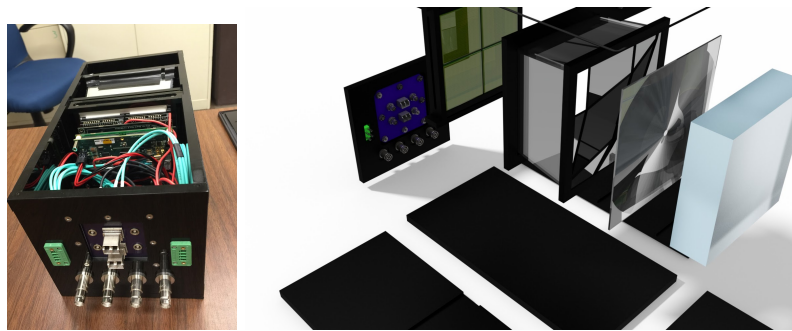


Figure 4: (left) The assembled mRICH prototype detector; (right) 3D rendering of the detector components.

3. Beam Test at Fermilab

The first prototype of the mRICH detector was tested at the Fermilab Test
50 Beam Facility (FTBF) under the T-1048 experiment in April of 2016. The T-
1048 experiment used the MTest beamline which has two modes of operation:
primary protons at 120 GeV and a secondary mixed beam consisting primarily
of pions, muons, and electrons with energies ranging from 1 GeV to 60 GeV
of either positive or negative charge. Given the short test period, the mRICH
55 detector was tested only with 120 GeV primary proton beam and the secondary
pion beam at 4 GeV and 8 GeV. The beam is delivered as a slow spill with a 4
second duration once per minute with a maximum intensity of a 10^5 particles
per spill. The momentum spread of the beam depends on the beam tune and is
 $\sim 3\%$. The beam spot size is also dependent of the beam energy and tune and
it ranges from ~ 6 mm to several centimeters in size.
60

The mRICH prototype detector was mounted at the center of a test stand
made from the extruded aluminum. Two sets of hodoscope (each consisting of
4 channels of horizontal 1 cm finger scintillator rods and 4 channels of vertical
rods) were mounted to the test stand at the front and the back to define the
65 incident particle position. The whole test assembly was put on a X-Y table for
aligning the detector with the particle beam. A beam event was triggered using
a pair of 7 cm-wide plastic scintillator paddles as shown in Fig. 5.



Figure 5: The mRICH test setup at the Fermilab Test Beam Facility.

4. Data Analysis and Results

Since the main goal of this prototype study is to test the working principles
 70 of the detector design and its performance, the analysis focused on the 120
 GeV primary proton beam test data set, because of its small beam size in order
 to clearly identify the ring image formed on the sensor plane. Figure 6 and
 Figure 7 show the accumulated ring image displays from the 120 GeV proton
 beam incident at the center of the mRICH and in the lower-left quadrant of the
 75 mRICH, respectively.

A ring ing algorithm, using a Circular Hough Transform [15], is developed
 in order to determine the radius of the Cherenkov ring image and the number
 of the Cherenkov photon on the even-by-event basis. The analysis results are
 summarized in Table 1 and 2. Both Cherenkov ring radius and number of
 80 photons found from the test beam data and from simulations agree with the
 analytical calculations.



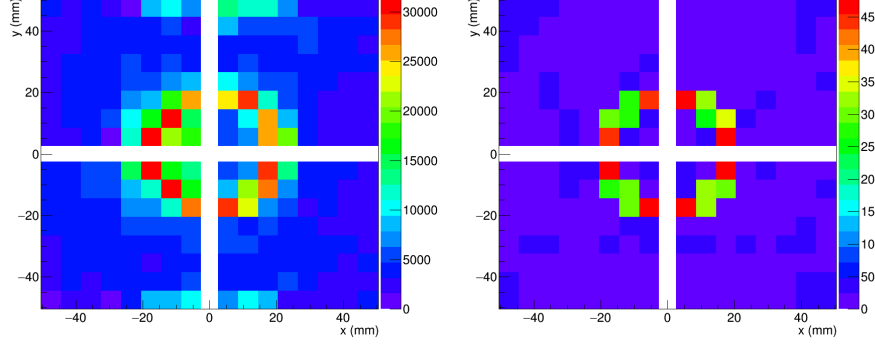


Figure 6: Accumulated ring image displays: (left) from 120 GeV proton beam incident toward the center of the mRICH; (right) from the matching Geant4 simulations. The blank regions are the gaps between the four Hamamatsu H12700 modules.

Table 1: The radius of the Cherenkov ring image and the number of Cherenkov photons at the sensor plane from 120 GeV proton beam incident toward the center of the mRICH.

	Analytical Calculation	Test Beam Data	Simulation
radius (mm)	19.4	19.0 ± 1.3	18.9 ± 1.0
total # of photons	10.4	11.0 ± 2.9	11.1 ± 2.9
# photons on ring		5.9 ± 1.8	5.8 ± 1.5

Table 2: The radius of the Cherenkov ring image and the number of Cherenkov photons at the sensor plane from 120 GeV proton beam incident toward the lower-left quadrant of the mRICH.

	Test Beam Data	Simulation
radius (mm)	20.8 ± 1.5	21.6 ± 0.9
total # of photons	17.6 ± 3.5	17.0 ± 3.4
# photons on ring	4.4 ± 1.0	4.4 ± 1.4

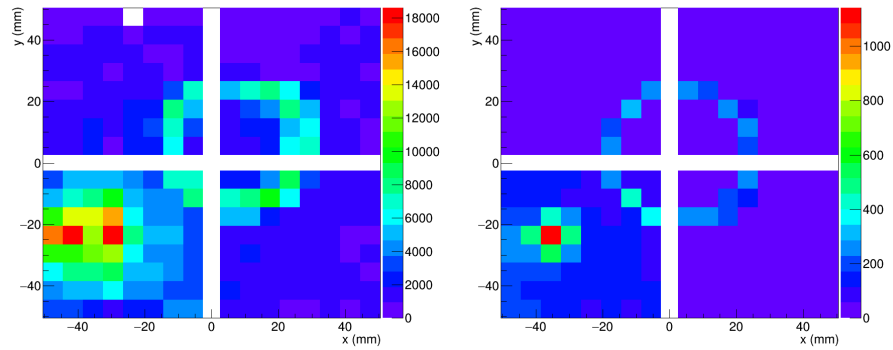


Figure 7: Accumulated ring image displays: (left) from 120 GeV proton beam incident toward the lower-left quadrant of the mRICH; (right) from the matching Geant4 simulations. The blank regions are the gaps between the four Hamamatsu H12700 modules.

5. Summary and Conclusion

A prototype of modular RICH detector has been successfully tested at Fermilab. The design features of this detector were well demonstrated with consistent results between test data, the detector simulation using Geant4, and the analytical calculations. After completing this initial validation, a new prototype is now under construction. This includes a 6-inch focal-length Fresnel lens and new Hamamatsu multi-anode PMTs with a pixel size of $3\text{ mm} \times 3\text{ mm}$, which should provide the resolution needed to demonstrate that the mRICH can satisfy the particle identification requirements of a future EIC detector.

6. Acknowledgements

We wish to thank the staff of the Fermilab Test Beam Facility for their assistance with T-1048 operation. We also want to thank the shop staff of the Physics Shop at Georgia State University for their assistance in constructing the prototype detector. This work was partially supported with the EIC R&D funding.

Appendix A. Analytical Calculation

In this appendix, we provide equations of the analytical calculations of the ring image radius and the number of Cherenkov photons at the sensor plane. See Fig. 2 for variable notations in the ray diagram.

The emission angle of Cherenkov radiation θ_c is given by

$$\theta_c = \cos^{-1} \frac{1}{\beta n}, \quad (\text{A.1})$$

where $\beta = \frac{v}{c}$ is the ratio of incident particle velocity to the speed of light inside the radiator, and n is index of refraction of aerogel. Considering the refraction at the interface between the aerogel and air, the refracted angle θ' of Cherenkov photon is

$$\theta' = \tan^{-1} \sqrt{\frac{n^2 \beta^2 - 1}{1 - (n^2 - 1)\beta^2}}, \quad (\text{A.2})$$

and the Cherenkov ring radius is

$$\begin{aligned} r &= f \cdot \tan \theta' \\ &= f \cdot \sqrt{\frac{n^2 \beta^2 - 1}{1 - (n^2 - 1)\beta^2}} \end{aligned} \quad (\text{A.3})$$

The number of photons emitted in the aerogel is

$$N_\gamma = 2\pi\alpha x \left(1 - \frac{1}{\beta^2 n^2}\right) \int_{\lambda_1}^{\lambda_2} \frac{d\lambda}{\lambda^2}. \quad (\text{A.4})$$

However, not all photons survive to reach to the photon sensor. Therefore, one should include the transmissions of each component. The number of surviving photons is

$$\begin{aligned} N_\gamma &= 2\pi\alpha x \left(1 - \frac{1}{\beta^2 n^2}\right) \\ &\times \int_{\lambda_1}^{\lambda_2} QE(\lambda) \cdot T_{aerogel}(\lambda) \cdot T_{lens}(\lambda) \cdot T_{glass\ window}(\lambda) \frac{d\lambda}{\lambda^2}, \end{aligned} \quad (\text{A.5})$$

where $QE(\lambda)$ is quantum efficiency of the H12700 photon sensor. $T_{aerogel}(\lambda)$, $T_{lens}(\lambda)$, and $T_{glass\ window}(\lambda)$ are the transmissions of aerogel block, Fresnel lens, and glass window at the front of photon sensor, respectively.

- [1] A. Aprahamian, et al., Reaching for the horizon: The 2015 long range plan
105 for nuclear science.
- [2] A. Accardi, et al., Electron-ion collider: The next qcd frontier, The European Physical Journal A 52 (9) (2016) 268. doi:10.1140/epja/i2016-16268-9.
URL <http://dx.doi.org/10.1140/epja/i2016-16268-9>
- 110 [3] E. Torassa, Particle identification with the {TOP} and {ARICH} detectors at belle {II}, Nuclear Instruments and Methods in Physics Research Section A: Accelerators, Spectrometers, Detectors and Associated Equipment 824 (2016) 152 – 155, frontier Detectors for Frontier Physics: Proceedings of the 13th Pisa Meeting on Advanced Detectors.
doi:<http://dx.doi.org/10.1016/j.nima.2015.11.016>.

- URL <http://www.sciencedirect.com/science/article/pii/S0168900215013789>
- [4] M. Tabata, et al., Silica aerogel radiator for use in the a-rich system utilized in the belle {II} experiment, Nuclear Instruments and Methods in Physics Research Section A: Accelerators, Spectrometers, Detectors and Associated Equipment 766 (2014) 212 – 216, {RICH2013} Proceedings of the Eighth International Workshop on Ring Imaging Cherenkov Detectors Shonan, Kanagawa, Japan, December 2-6, 2013. doi:<http://dx.doi.org/10.1016/j.nima.2014.04.030>.
- 120 URL <http://www.sciencedirect.com/science/article/pii/S0168900214004264>
- [5] M. Adinolfi, et al., Performance of the lhcb rich detector at the lhc, The European Physical Journal C 73 (5) (2013) 2431. doi:[10.1140/epjc/s10052-013-2431-9](https://doi.org/10.1140/epjc/s10052-013-2431-9).
- 130 URL <http://dx.doi.org/10.1140/epjc/s10052-013-2431-9>
- [6] T. L. Collaboration, A. A. A. Jr, et al., The lhcb detector at the lhc, Journal of Instrumentation 3 (08) (2008) S08005.
- URL <http://stacks.iop.org/1748-0221/3/i=08/a=S08005>
- [7] J. Engelfried, et al., {SELEX} {RICH} performance and physics results, Nuclear Instruments and Methods in Physics Research Section A: Accelerators, Spectrometers, Detectors and Associated Equipment 502 (1) (2003) 285 – 288, experimental Techniques of Cherenkov Light Imaging. Proceedings of the Fourth International Workshop on Ring Imaging Cherenkov Detectors. doi:[http://dx.doi.org/10.1016/S0168-9002\(03\)00289-4](http://dx.doi.org/10.1016/S0168-9002(03)00289-4).
- 135 URL <http://www.sciencedirect.com/science/article/pii/S0168900203002894>
- [8] J. Engelfried, et al., The {SELEX} phototube {RICH} detector, Nuclear Instruments and Methods in Physics Research Section A: Accelerators, Spectrometers, Detectors and Associated Equipment 431 (1–2) (1999) 53

- 145 – 69. doi:[http://dx.doi.org/10.1016/S0168-9002\(99\)00043-1](http://dx.doi.org/10.1016/S0168-9002(99)00043-1).
 URL <http://www.sciencedirect.com/science/article/pii/S0168900299000431>
- [9] M. Contalbrigo, E. Cisbani, P. Rossi, The {CLAS12} large area {RICH} detector, Nuclear Instruments and Methods in Physics Research Section A: Accelerators, Spectrometers, Detectors and Associated Equipment 639 (1) (2011) 302 – 306, proceedings of the Seventh International Workshop on Ring Imaging Cherenkov Detectors.
 150 doi:<http://dx.doi.org/10.1016/j.nima.2010.10.047>.
 URL <http://www.sciencedirect.com/science/article/pii/S0168900210022862>
 155
- [10] R. A. Montgomery, A ring imaging cherenkov detector for {CLAS12}, Nuclear Instruments and Methods in Physics Research Section A: Accelerators, Spectrometers, Detectors and Associated Equipment 732 (2013) 366 – 370, vienna Conference on Instrumentation 2013.
 160 doi:<http://dx.doi.org/10.1016/j.nima.2013.08.012>.
 URL <http://www.sciencedirect.com/science/article/pii/S0168900213011388>
- [11] D. Fields, H. van Hecke, J. Boissevain, B. Jacak, W. Sondheim, J. Sullivan, W. Willis, K. Wolf, E. Noteboom, P. Peters, R. Burke,
 165 Use of aerogel for imaging cherenkov counters, Nuclear Instruments and Methods in Physics Research Section A: Accelerators, Spectrometers, Detectors and Associated Equipment 349 (2) (1994) 431 – 437.
 doi:[http://dx.doi.org/10.1016/0168-9002\(94\)91207-6](http://dx.doi.org/10.1016/0168-9002(94)91207-6).
 URL <http://www.sciencedirect.com/science/article/pii/0168900294912076>
 170
- [12] J. Allison, et al., Recent developments in geant4, Nuclear Instruments and Methods in Physics Research Section A: Accelerators, Spectrometers, Detectors and Associated Equipment 835 (2016) 186 – 225.

- doi:<http://dx.doi.org/10.1016/j.nima.2016.06.125>.
- 175 URL <http://www.sciencedirect.com/science/article/pii/S0168900216306957>
- [13] C. Lippmann, Particle identification, Nuclear Instruments and Methods in Physics Research Section A: Accelerators, Spectrometers, Detectors and Associated Equipment 666 (2012) 148 – 172, advanced Instrumentation.
- 180 doi:<http://dx.doi.org/10.1016/j.nima.2011.03.009>.
- URL <http://www.sciencedirect.com/science/article/pii/S0168900211005419>
- [14] Edmund Optics, Specification of Fresnel Lens (stock no. 32–593).
- 185 URL <http://www.edmundoptics.com/optics/optical-lenses/fresnel-lenses/fresnel-lenses/32593/>
- [15] E. E. Zelniker, I. V. L. Clarkson, Maximum-likelihood estimation of circle parameters via convolution, IEEE Transactions on Image Processing 15 (4) (2006) 865–876.